



A New Approach on Solving One-Mass Model of Vocal Cord using Hybrid Cubic B-Spline Collocation Method

Nur Fatin Amirah Mohd Rodzi¹, Shazalina Mat Zin^{1*}, Syatirah Mat Zin², Muhammad Abbas³

¹ Institute of Engineering Mathematics, Universiti Malaysia Perlis (UniMAP), 02600 Arau, Perlis, Malaysia

² Department of Dental Science, Advanced Medical and Dental Institute, Universiti Sains Malaysia, 13200 Kepala Batas, Pulau Pinang, Malaysia

³ Department of Mathematics, University of Sargodha, PAF Road, 40100 Sargodha, Pakistan

ABSTRACT

The vocal cords, also known as vocal folds, are responsible for producing sound and creating the voice. In this work, hybrid cubic B-spline collocation method (HCBs) and ode45 built-in solver in MATLAB were applied to solve one-mass model of vocal cord numerically. From the model, displacements were generated by analysing the voice recording samples of 109 healthy participants. Based on the recordings, the frequency of each sample was accumulated and utilized in displacements calculation. In order to verify the value of displacements, absolute error and maximum error were calculated. The numerical results were indicated that HCBs generate closer displacement with ode45. The error was shown that HCBs could be reliable method and produce accurate displacement of one-mass model of vocal cord.

Keywords:

Hybrid cubic B-spline; Vocal cord displacement; One-mass model

1. Introduction

Speech production is made possible by the vocal cords, which are located in the larynx, or voice box. As air is expelled from the lungs and travels upwards through the trachea, it passes over the vocal cords, causing them to vibrate. This vibration creates sound, which is then modulated by the tongue, lips, and other articulators, allowing human to produce a wide range of speech sounds. The vocal cords play a crucial role in this process, as their ability to rapidly and accurately vibrate determines the quality and clarity of spoken words. The first model of vocal cord is one-mass model of vocal cord by Flanagan and Landgraf in 1968 [1] which then evolved to two-mass model by Ishizaka and Flanagan [2] and Guasch *et al.*, [3]. Two-mass model consider both vocal cord by two equation that represented both measurements. Further years later, Titze produced a model with 16 mass [4,5] and three-mass model was also investigated by other authors in 1993 [6,7]. The wide spread of vocal cord model has increased the study of vocal cord characteristics such as vibrations [8,9], collisions [10,11], self-oscillation [12,13] and aerodynamics [14].

* Corresponding author.

E-mail address: shazalina@unimap.edu.my

<https://doi.org/10.37934/araset.59.2.2029>

Numerical method studies began to develop from one-dimensional model [15] to three-dimensional model [16] of mechanical model and commonly solved by using finite element method [17]. These models also heavily aided in the analysis of vocal cord by using numerical and analytical method. Finite element is one of the numerical methods that are usually utilized in solving vocal cord model other than analytical method. Analytical method was less utilized as the method consumed more time than numerical method and sometimes fails to maintain its pace with large or complex value. Some authors that investigated vocal cord model by using finite element were Gunter [18], Vampola *et al.*, [7] and Hermant *et al.*, [19]. Throughout previous years, many works have been done exploring B-spline, trigonometric B-spline and hybrid B-spline for solving initial and boundary value problem of a differential equations numerically [20-24]. Since the ability of those methods have been proven, HCBs will be proposed to solve an initial value problem of one-mass model of vocal cord.

In this work, the 109 recording samples of healthy participant gathered from Walden [25] were used to approximate the displacement of vocal cord. From each sample, the frequencies will be generated by Origin software, which is a software that could analysed the real voices recording. Average of the frequencies has been calculated and applied to solve one-mass model of vocal cord. The aim of this work is to generate displacement of one-mass mechanical model of vocal cord using HCBs and ode45 numerically. Then, the generated displacements will be compared and discussed

1.1 One-Mass Model of Vocal Cord

In this section, one-mass model proposed of vocal cord will be introduced. This model considered vocal cord as a spring-mass-damper system which is visually depict in Figure 1. Mathematically, the model is given by

$$mx'' + bx' + kx = F \quad (1)$$

where m is mass, b is viscous damping, k is spring constant, F is forcing function of the system and x represent displacement of the mass at time t . The value of b and k are calculated by

$$b = 2\sqrt{mk} \quad \text{and} \quad k = 4\pi^2 m (f_0)^2 \quad (2)$$

where f_0 is fundamental frequency. In order to solve Eq. (1), the following initial conditions are considered

$$x(t_0) = \alpha \quad \text{and} \quad x'(t_0) = \beta \quad (3)$$

where α and β are constant values. The forcing function of the system is depending on time and can be written as

$$F(t) = \frac{1}{2}(P_1 + P_2)(ld) \quad (4)$$

with l and d are the vocal cord length and thickness, respectively. The P_1 and P_2 are the inlet and outlet of glottal orifice of vocal cord which is given by

$$P_1 = (P_s - 1.37 P_B) \text{ and } P_2 = -0.50 P_B \quad (5)$$

where P_s represented subglottal pressure while P_B represent the value of Bernoulli pressure, $P_B = \frac{1}{2} \rho |U_g|^2 A_g^{-2}$. In Bernoulli pressure equation, ρ represent the air density, A_g is the area of glottal orifice and U_g is the acoustic volume velocity through the glottal orifice.

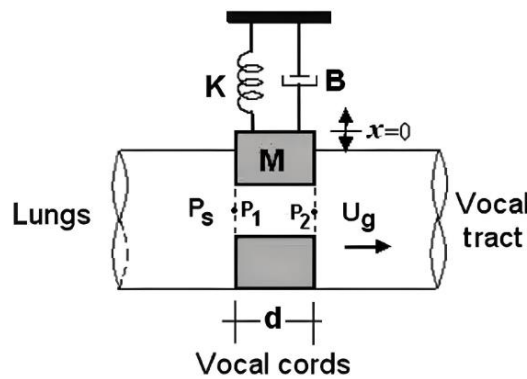


Fig. 1. Mechanical model of vocal cords [1,15]

2. Methodology

2.1 Hybrid Cubic B-Spline Collocation Method (HCBs)

In this section, the methodology to solve Eq. (1) using HCBs is discussed. The approximate solution of one-mass model of vocal cord is defined as

$$x(t_j) = \sum_{j=-3}^{n-1} C_j H_j^4(t) \quad (6)$$

with C_j is unknown to be determined and $H_j^4(t)$ is HCBs basis function which given by

$$H_j^4(t) = (\gamma) B_j^4(t) + (1-\gamma) T_j^4(t) \quad (7)$$

where $0 < \gamma < 1$. The $B_j^4(t)$ and $T_j^4(t)$ are represented as

$$B_j^4(t) = \frac{1}{6h^3} \begin{cases} (t-t_j)^3, & t \in [t_j, t_{j+1}] \\ h^3 + 3h^2(t_{j+1}) + 3h^2(t-t_{j+1}) - 3(t-t_{j+1})^3, & t \in [t_{j+1}, t_{j+2}] \\ h^3 + 3h^2(t_{j+3}-t) + 3h(t_{j+3}-t)^2 - 3(t_{j+3}-t)^3, & t \in [t_{j+2}, t_{j+3}] \\ (t_{j+4}-t)^3, & t \in [t_{j+3}, t_{j+4}] \end{cases} \quad (8)$$

and

$$T_j^4(t) = \frac{1}{\theta} \begin{cases} \sigma^3(t_j), & t \in [t_j, t_{j+1}] \\ (t_j)[\sigma(t_j)\delta(t_{j+2}) + \delta(t_{j+3})\sigma(t_{j+1})] + \delta(t_{j+4})\sigma^2(t_{j+1}), & t \in [t_{j+1}, t_{j+2}] \\ \sigma(t_j)\delta(t_{j+3}) + \delta(t_{j+4})[\sigma(t_{j+1})\delta(t_{j+3}) + \delta(t_{j+3})\sigma(t_{j+2})], & t \in [t_{j+2}, t_{j+3}] \\ \delta^3(t_{j+4}), & t \in [t_{j+3}, t_{j+4}] \end{cases} \quad (9)$$

respectively, where $\sigma(t_j) = \sin\left(\frac{t-t_j}{2}\right)$, $\delta(t_j) = \sin\left(\frac{t_j-t}{2}\right)$, and $\theta = \sin\left(\frac{h}{2}\right)\sin(h)\sin\left(\frac{3h}{2}\right)$. Eq. (7) become cubic B-spline and trigonometric cubic B-spline when $\gamma = 1$ and $\gamma = 0$, respectively.

There are only three nonzero basis function; $H_{j-3}^4(t_j)$, $H_{j-2}^4(t_j)$ and $H_{j-1}^4(t_j)$, are included over subinterval $[t_j, t_{j+1}]$. By considering those nonzero basis functions, Eq. (6) and its derivatives can be simplified and returned as

$$\begin{aligned} x(t_j) &= D_1 C_{j-3} + D_2 C_{j-2} + D_1 C_{j-1}, \\ x'(t_j) &= D_3 C_{j-3} - D_3 C_{j-1}, \\ x''(t_j) &= D_4 C_{j-3} + D_5 C_{j-2} + D_4 C_{j-1} \end{aligned} \quad (10)$$

with $D_i = \gamma\eta_i + (1-\gamma)\zeta_i$ for $i=1,2,\dots,5$ where $\eta_1 = \frac{1}{6}$, $\eta_2 = \frac{4}{6}$, $\eta_3 = \frac{1}{2h}$, $\eta_4 = \frac{1}{h^2}$, $\eta_5 = \frac{2}{h^2}$, $\zeta_1 = \frac{k_1^2}{k_2 k_3}$, $\zeta_2 = \frac{2k_1}{k_3}$, $\zeta_3 = \frac{-3}{4k_3}$, $\zeta_4 = \frac{3(k_1 - 2k_1^3 + k_3)}{8k_1 k_2 k_3}$, $\zeta_5 = \frac{-3(k_4 + k_1^2 k_2)}{4k_1 k_2 k_3}$, $k_1 = \sin\left(\frac{h}{2}\right)$, $k_2 = \sin(h)$, $k_3 = \sin\left(\frac{3h}{2}\right)$ and $k_4 = \sin(2h)$.

In order to solve Eq. (1), Eq. (10) is then substituted into the equation to produce a matrix system of order $(n+1)$ equation with $(n+3)$ unknown. Two equations are needed to generate a unique solution. Further, initial condition which given in Eq. (3) is approximated and represented as

$$\begin{aligned} x(t_0) &= D_1 C_{j-3} + D_2 C_{j-2} + D_1 C_{j-1} = \alpha, \\ x'(t_0) &= D_3 C_{j-3} - D_3 C_{j-1} = \beta. \end{aligned} \quad (11)$$

Eq. (11) is added to the system and become

$$[\mathbf{A}]_{(n+3) \times (n+3)} \cdot [\mathbf{C}]_{(n+3) \times 1} = [\mathbf{R}]_{1 \times (n+3)} \quad (12)$$

$$\text{where } \mathbf{A} = \begin{bmatrix} D_1 & D_2 & D_1 & 0 & \dots & \dots & \dots & 0 \\ \omega_1 & \omega_2 & \omega_3 & 0 & \dots & \dots & \dots & 0 \\ 0 & \omega_1 & \omega_2 & \omega_3 & 0 & \dots & \dots & 0 \\ \vdots & 0 & \omega_1 & \omega_2 & \omega_3 & 0 & \dots & 0 \\ 0 & \dots & \ddots & \ddots & \ddots & \dots & \dots & 0 \\ 0 & \dots & \dots & \dots & 0 & \omega_1 & \omega_2 & \omega_3 \\ D_3 & 0 & D_3 & 0 & \dots & \dots & \dots & 0 \end{bmatrix}, \quad \mathbf{C} = \begin{bmatrix} C_{-3} \\ C_{-2} \\ C_{-1} \\ \vdots \\ C_{n-1} \end{bmatrix} \quad \text{and} \quad \mathbf{F} = \begin{bmatrix} \alpha \\ F \\ \vdots \\ F \\ \beta \end{bmatrix} \quad \text{with}$$

$\omega_1 = m(D_4) + b(D_3) + k(D_1)$, $\omega_2 = m(D_5) + k(D_2)$ and $\omega_3 = m(D_4) + b(-D_3) + k(D_1)$. By solving the matrix system, \mathbf{C} is generated and substituted into Eq. (6) to obtain the approximate solution of Eq. (1) or also known as approximate displacement of vocal cord.

2.2 Ode45 Built-in Solver

By using the same parameter as HCBS, Eq. (1) is also solved by using a build-in solver in MATLAB called ode45 as follows:

```
f = @(t,x) [x(2); (F-r*x(2)-k*x(1))/m];
tspan=t0:(0.05-0)/(n):tN;
ts = zeros(1,n); xs = zeros(1,n);
[ts,xs] = ode45(f,tspan,[0;0]);
```

3. Results and Discussion

In this section, the generated displacements of vocal cord by using HCBs and ode45 are analysed and compared. Two values of γ for HCBs are considered as $\gamma = 0.30$ and $\gamma = 0.99$. The parameters used are shown in Table 1. The frequency value, f_0 , is chosen from the average frequency of voice recording samples. Otherwise, the parameters are mostly referred from Flanagan and Landgraf [1] and Cataldo *et al.*, [15].

Table 1
 Parameters value used in solving Eq. (1)

Parameter	Value
m	0.240×10^{-3} kg
b	0.667 Ns/m
k	4.925×10^5 Ns/m
t	0.050 s
P_{s0}	783 Pa
ρ	1.300×10^3 kg/m ³
l	1.800×10^{-2} m
d	0.300×10^{-3} m
f_0	228 Hz
h	1.000×10^{-4}

3.1 HCBs ($\gamma = 0.30$) and Ode45

In this subsection, the generated displacement by HCBs ($\gamma = 0.30$) and ode45 is displayed and tabulated. Figure 2 shows graph of generated displacement by HCBs ($\gamma = 0.30$) and ode45.

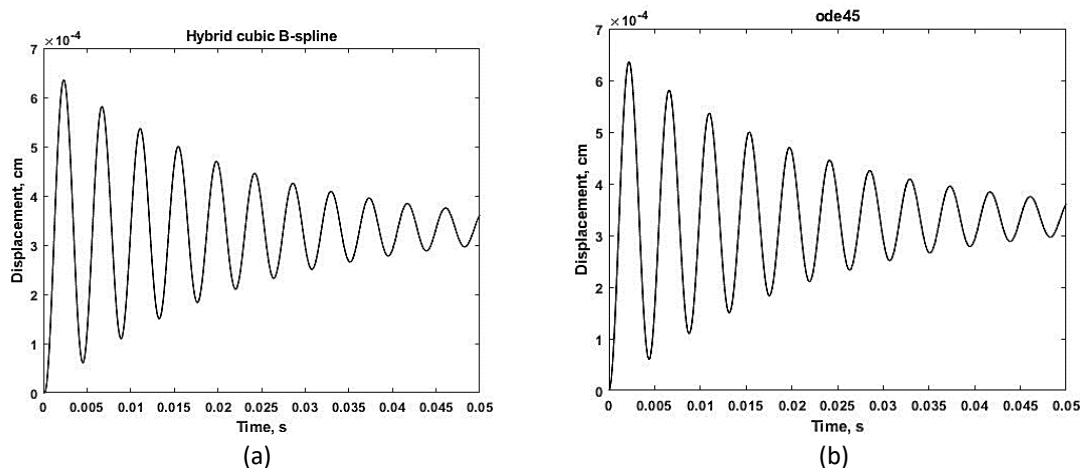


Fig. 2. Generated displacements by a) HCBs with $\gamma = 0.30$ and b) ode45

Meanwhile, the numerical data of both method within 0.05 s is listed and compared in Table 2. The data shows that the generated displacement by HCBs agreed well with the generated displacement by ode45.

Table 2

Generated displacement solved by ode45 (x -ode45) and HCBs (x - hybrid) with $\gamma = 0.30$ within 0.050 s

Time (s)	x -ode45 (cm)	x -hybrid (cm)
0.010	3.5399×10^{-4}	3.6302×10^{-4}
0.015	4.7113×10^{-4}	4.7732×10^{-4}
0.020	4.6581×10^{-4}	4.6291×10^{-4}
0.025	3.8562×10^{-4}	3.7531×10^{-4}
0.030	3.0445×10^{-4}	3.9434×10^{-4}
0.035	2.6992×10^{-4}	2.6679×10^{-4}
0.040	2.8515×10^{-4}	2.8999×10^{-4}
0.045	3.2317×10^{-4}	3.3141×10^{-4}
0.050	3.5357×10^{-4}	3.5926×10^{-4}

3.2 HCBs ($\gamma = 0.99$) and Ode45

The generated displacement by HCBs with $\gamma = 0.99$ and ode45 are presented in Figure 3.

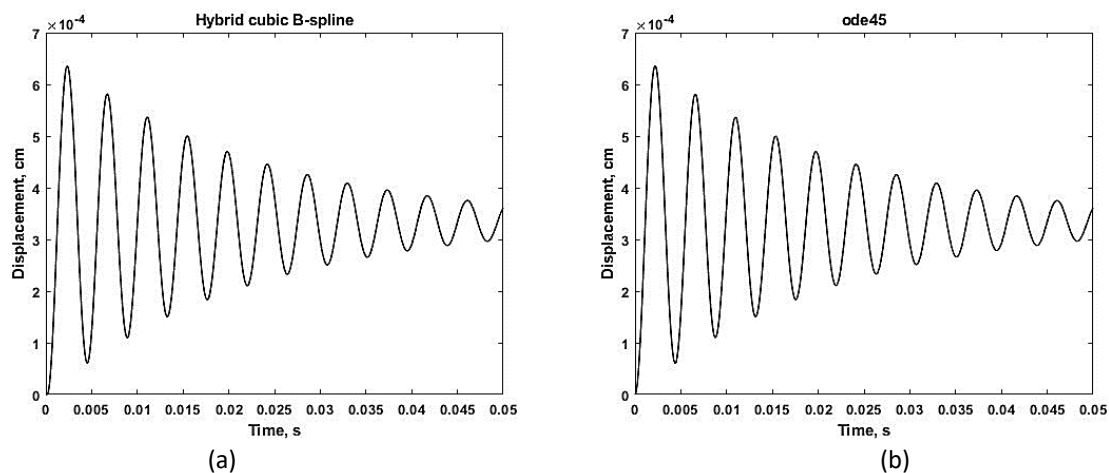


Fig. 3. Generated displacements by a) HCBs with $\gamma = 0.99$ and b) ode45

Table 3 tabulates the generated displacement of both method within 0.050 s. Based on the results, it can be seen that the HCBs of $\gamma = 0.99$ could also performed well compared to HCBs of $\gamma = 0.30$.

Table 3

Generated displacement solved by ode45 (x -ode45) and HCBs (x - hybrid) with $\gamma = 0.99$ within 0.050 s

Time (s)	x-ode45 (cm)	x -hybrid (cm)
0.010	3.5399×10^{-4}	3.6302×10^{-4}
0.015	4.7113×10^{-4}	4.7732×10^{-4}
0.020	4.6581×10^{-4}	4.6291×10^{-4}
0.025	3.8562×10^{-4}	3.7531×10^{-4}
0.030	3.0445×10^{-4}	2.9433×10^{-4}
0.035	2.6992×10^{-4}	2.6679×10^{-4}
0.040	2.8515×10^{-4}	2.8999×10^{-4}
0.045	3.2317×10^{-4}	3.3141×10^{-4}
0.050	3.5357×10^{-4}	3.5929×10^{-4}

In order to compare the displacements of HCBs of $\gamma = 0.30$ and $\gamma = 0.99$, the maximum displacement from Table 2 and Table 3 are gathered in Table 4. It can be observed that maximum displacement is at $t = 0.015$ s which is presented in Table 4. The obtained displacements in Table 4 also shows that $\gamma = 0.99$ has slightly lower maximum displacement than $\gamma = 0.30$. Since ode45 has the maximum displacement of 4.7113×10^{-4} cm, this interprets that $\gamma = 0.99$ has closer value of maximum displacement to ode45 than $\gamma = 0.30$.

Table 4

Maximum displacement (x -max) generated by HCBs with $\gamma = 0.30$ and $\gamma = 0.99$

γ	Time (s)	x -max (cm)
0.30	0.015	$4.77324816 \times 10^{-4}$
0.99	0.015	$4.77324815 \times 10^{-4}$

3.3 Absolute Error Obtained by HCBs Compared to Ode45

This subsection calculates the absolute error and maximum error by comparing the generated displacement by HCBs and ode45. The formula is considered as the following equations:

$$\text{Absolute error} = |\bar{x}_i - x_i|, \tag{13}$$

$$\text{Maximum error} = L_\infty = \max|\bar{x}_i - x_i|, \tag{14}$$

where \bar{x}_i is generated displacements by ode45 and x_i generated displacements by HCBs.

Table 5 list the absolute errors within 0.050 s. Meanwhile the maximum error obtained by HCBs with $\gamma = 0.30$ and $\gamma = 0.99$ is tabulated in Table 6. Based on Table 5, it can be seen that $\gamma = 0.99$ obtained smaller error than $\gamma = 0.30$.

Table 5
 Absolute errors obtained by HCBs with $\gamma = 0.30$ and $\gamma = 0.99$ within 0.050 s

Time (s)	Absolute error	
	$\gamma = 0.30$	$\gamma = 0.99$
0.010	9.0351910×10^{-6}	9.0351889×10^{-6}
0.015	6.1986152×10^{-6}	6.1986139×10^{-6}
0.020	2.8956127×10^{-6}	2.8956117×10^{-6}
0.025	1.0312675×10^{-5}	1.0312673×10^{-5}
0.030	1.0117635×10^{-5}	1.0117632×10^{-5}
0.035	3.1378975×10^{-6}	3.1378972×10^{-6}
0.040	4.8454254×10^{-6}	4.8454240×10^{-6}
0.045	8.2377835×10^{-6}	8.2377816×10^{-6}
0.050	5.6899366×10^{-6}	5.6899355×10^{-6}

From Table 6, it can be observed that $\gamma = 0.99$ has obtained smaller maximum error than $\gamma = 0.30$. Overall, the numerical data of Table 5 and 6 suggest that $\gamma = 0.99$ generate closer displacement to ode45 in solving one-mass model of vocal cord than $\gamma = 0.30$.

Table 6
 Maximum error obtained by HCBs with $\gamma = 0.30$ and $\gamma = 0.99$

γ	Time (s)	Maximum error
0.30	0.025	1.0312675×10^{-5}
0.99	0.025	1.0312673×10^{-5}

4. Conclusions

In conclusion, one-mass model of vocal cord has successfully solved by using HCBs collocation method. The numerical results indicate that HCBs has generated displacement with closer value to ode45. The calculated errors shown that HCBs produce accurate displacement of vocal cord could be reliable numerical method in solving one-mass model of vocal cord.

Acknowledgement

The authors would like to acknowledge the support from the Fundamental Research Grant Scheme (FRGS) under a grant number of FRGS/1/2019/STG06/UNIMAP/03/2 from the Ministry of Higher Education of Malaysia.

References

- [1] Flanagan, J., and Lois Landgraf. "Self-oscillating source for vocal-tract synthesizers." *IEEE Transactions on Audio and Electroacoustics* 16, no. 1 (1968): 57-64. <https://doi.org/10.1109/TAU.1968.1161949>
- [2] Ishizaka, Kenzo, and James L. Flanagan. "Synthesis of voiced sounds from a two-mass model of the vocal cords." *Bell system technical journal* 51, no. 6 (1972): 1233-1268. <https://doi.org/10.1002/j.1538-7305.1972.tb02651.x>
- [3] Guasch, Oriol, Annemie Van Hirtum, A. Inés Fernández, and Marc Arnela. "Controlling chaotic oscillations in a symmetric two-mass model of the vocal folds." *Chaos, Solitons & Fractals* 159 (2022): 112188. <https://doi.org/10.1016/j.chaos.2022.112188>
- [4] Titze, Ingo R. "The human vocal cords: A mathematical model: Part I." *Phonetica* 28, no. 3-4 (1973): 129-170. <https://doi.org/10.1159/000259453>
- [5] Titze, Ingo R. "The human vocal cords: A mathematical model." *Phonetica* 29, no. 1-2 (1974): 1-21. <https://doi.org/10.1159/000259461>
- [6] Story, Brad H., and Ingo R. Titze. "Voice simulation with a body-cover model of the vocal folds." *The Journal of the Acoustical Society of America* 97, no. 2 (1995): 1249-1260. <https://doi.org/10.1121/1.412234>
- [7] Vampola, Tomáš, Jaromír Horáček, and Ivo Klepáček. "Computer simulation of mucosal waves on vibrating human vocal folds." *Biocybernetics and biomedical engineering* 36, no. 3 (2016): 451-465. <https://doi.org/10.1016/j.bbe.2016.03.004>
- [8] Rocha, Raissa Bezerra, Wamberto José Lira de Queiroz, and Marcelo Sampaio de Alencar. "Voice production model based on phonation biophysics." *EURASIP Journal on Advances in Signal Processing* 2021, no. 1 (2021): 78. <https://doi.org/10.1186/s13634-021-00746-2>
- [9] Suryadi, Aji. "Numerical Analysis and Optimization Research on Backflow Effect of Nitrogen Compressor Piping System Based on Vibration Data." *Journal of Advanced Research in Applied Mechanics* 78, no. 1 (2021): 1-12.
- [10] Tao, Chao, Jack J. Jiang, and Yu Zhang. "Simulation of vocal fold impact pressures with a self-oscillating finite-element model." *The Journal of the Acoustical Society of America* 119, no. 6 (2006): 3987-3994. <https://doi.org/10.1121/1.2197798>
- [11] Mora, Luis A., Hector Ramirez, Juan I. Yuz, Yann Le Gorec, and Matías Zaňartu. "Energy-based fluid–structure model of the vocal folds." *IMA Journal of Mathematical Control and Information* 38, no. 2 (2021): 466-492. <https://doi.org/10.1093/imamci/dnaa031>
- [12] Horáček, J., P. Šidlof, and J. G. Švec. "Numerical simulation of self-oscillations of human vocal folds with Hertz model of impact forces." *Journal of fluids and structures* 20, no. 6 (2005): 853-869. <https://doi.org/10.1016/j.jfluidstructs.2005.05.003>
- [13] Hájek, Petr, Pavel Švancara, Jaromír Horáček, and Jan G. Švec. "Finite-element modeling of vocal fold self-oscillations in interaction with vocal tract: Comparison of incompressible and compressible flow model." (2021). <https://doi.org/10.24132/acm.2021.672>
- [14] Motie-Shirazi, Mohsen, Matías Zaňartu, Sean D. Peterson, and Byron D. Erath. "Vocal fold dynamics in a synthetic self-oscillating model: Intraglottal aerodynamic pressure and energy." *The Journal of the Acoustical Society of America* 150, no. 2 (2021): 1332-1345. <https://doi.org/10.1121/10.0005882>
- [15] Cataldo, Edson, Fabiana R. Leta, Jorge Lucero, and Lucas Nicolato. "Synthesis of voiced sounds using low-dimensional models of the vocal cords and time-varying subglottal pressure." *Mechanics Research Communications* 33, no. 2 (2006): 250-260. <https://doi.org/10.1016/j.mechrescom.2005.05.007>
- [16] Wang, Xiaojian, Weili Jiang, Xudong Zheng, and Qian Xue. "A computational study of the effects of vocal fold stiffness parameters on voice production." *Journal of Voice* 35, no. 2 (2021): 327-e1. <https://doi.org/10.1016/j.jvoice.2019.09.004>
- [17] Palaparathi, Anil, Simeon Smith, Ted Mau, and Ingo R. Titze. "A computational study of depth of vibration into vocal fold tissues." *The Journal of the Acoustical Society of America* 145, no. 2 (2019): 881-891. <https://doi.org/10.1121/1.5091099>
- [18] Gunter, Heather E. "A mechanical model of vocal-fold collision with high spatial and temporal resolution." *The Journal of the Acoustical Society of America* 113, no. 2 (2003): 994-1000. <https://doi.org/10.1121/1.1534100>

- [19] Hermant, Nicolas, Franz Chouly, Fabrice Silva, and Paul Luizard. "Numerical study of the vibrations of an elastic container filled with an inviscid fluid." *ZAMM-Journal of Applied Mathematics and Mechanics/Zeitschrift für Angewandte Mathematik und Mechanik* 98, no. 4 (2018): 602-621. <https://doi.org/10.1002/zamm.201600208>
- [20] Gholamian, Mohammad, and Jafar Saberi-Nadjafi. "Cubic B-splines collocation method for a class of partial integro-differential equation." *Alexandria engineering journal* 57, no. 3 (2018): 2157-2165. <https://doi.org/10.1016/j.aej.2017.06.004>
- [21] Heilat, Ahmed Salem, Nur Nadiyah Abd Hamid, and Ahmad Izani Md Ismail. "Extended cubic B-spline method for solving a linear system of second-order boundary value problems." *SpringerPlus* 5, no. 1 (2016): 1314. <https://doi.org/10.1186/s40064-016-2936-4>
- [22] Rabah, Ahlem Ben, Shaher Momani, and Omar Abu Arqub. "The B-spline collocation method for solving conformable initial value problems of non-singular and singular types." *Alexandria Engineering Journal* 61, no. 2 (2022): 963-974. <https://doi.org/10.1016/j.aej.2021.06.011>
- [23] Zin, Shazalina Mat. "Hybrid cubic B-spline collocation method for solving one-dimensional wave equation." In *AIP Conference Proceedings*, vol. 1775, no. 1. AIP Publishing, 2016. <https://doi.org/10.1063/1.4965204>
- [24] Mat Zin, Shazalina, Ahmad Abd Majid, Ahmad Izani Md Ismail, and Muhammad Abbas. "Application of Hybrid Cubic B-Spline Collocation Approach for Solving a Generalized Nonlinear Klien-Gordon Equation." *Mathematical Problems in Engineering* 2014, no. 1 (2014): 108560. <https://doi.org/10.1155/2014/108560>
- [25] Walden, Patrick R. "Perceptual voice qualities database (PVQD): database characteristics." *Journal of Voice* 36, no. 6 (2022): 875-e15. <https://doi.org/10.1016/j.jvoice.2020.10.001>